catalysts

MDPI

Article

Base-Free Selective Oxidation of Glycerol over LDH Hosted Transition Metal Complexes Using 3% H_2O_2 as Oxidant

Xiaoli Wang [1], Congxiao Shang [2], Gongde Wu [1,*], Xianfeng Liu [1] and Hao Liu [1]

[1] Department of Environment and Technology, Nanjing Institute of Technology, Nanjing 211167, China; wangxiaoli212@njit.edu.cn (X.W.); liuxianfeng@njit.edu.cn (X.L.); liuhao@163.com (H.L.)

[2] School of Environment Science, University of East Angelia, Norwich NR4 7TJ, UK; c.shang@uea.ac.uk

* Correspondence: wugongde@njit.edu.cn; Tel./Fax: +86-25-8611-8960

Academic Editor: Xiao-Feng Wu

Received: 9 June 2016; Accepted: 12 July 2016; Published: 15 July 2016

Abstract: A series of transition metal sulphonato-Schiff base complexes were intercalated into Mg–Al layered-double hydroxides (LDHs). The obtained catalysts were characterized by FTIR, XRD, N_2 sorption, SEM and elemental analysis, and then were used in the selective oxidation of glycerol (GLY) using 3% H_2O_2 as an oxidant. It was found that their catalytic performances were closely related to the loading of active complexes, the Schiff base ligands and the metal centers of the catalysts, as well as the reaction conditions. The optimal conversion of GLY was 85.0%, while the selectivity of 1,3-dihydroxyacetone (DHA) was 56.5%. Moreover, the catalysts could be reused at least 10 times.

Keywords: LDH; transition metal; selective oxidation; GLY; DHA

1. Introduction

The use of biorenewable feedstocks to produce commodity chemicals and clean fuels as a substitute for the limited fossil fuel reserves is an essential pathway to sustainable development [1,2]. In this context, the biodiesel industry was booming in the past decades. However, as an unavoidable by-product of biodiesel production, 1 mol GLY is formed during the generation of every 3 mol biodiesel methyl esters. So, the effective use of GLY has attracted much attention in academia and industry. Luckily, as a highly functionalized molecule, GLY can produce various valuable compounds by oxidation, dehydration, hydrogenolysis, esterification, transesterificaiton, polymerization, and so on. Among them, the oxidation conversion is of immense current importance for the synthesis of fine chemicals with high added value such as DHA, glyceric acid, glyceraldehyde, hydroxypyruvic acid, mesooxalic acid and tartronic acid. Particularly, DHA is one of the most valuable products due to its great demand in cosmetics [3,4]. However, owing to the three hydroxyl groups in GLY, the selective oxidation of GLY to DHA is a crucial dilemma from the point of view of catalyst design.

In the past decades, there were many successful reports on the selective oxidation of GLY using noble metal catalysts [5–12]. However, due to the high cost and easy catalyst deactivation of noble metal catalysts, the design of efficient transition metal catalysts was becoming a hot point in the current research area [1,13–20]. Zhou et al. reported that Cu-containing hydrotalcites were active catalysts in the selective oxidation of GLY to glyceric acid, and the highest yield reached 68% [1]. Crotti et al. and Shul'pin et al. found that iron complexes and manganese complexes could catalytically oxidize GLY to DHA, respectively (Yield < 15%) [13,18]. Although several promising transition metal catalysts have been reported, the activity and selectivity of catalysts still need to be improved. Thus, it was of significance to design highly effective catalysts, especially a low-cost heterogeneous catalyst, for the oxidation reaction of GLY.

LDHs were often considered as catalysts or catalyst supports owing to their adjustable surface basicity, high surface and thermal stability, along with the adjustable variability of their laminate cations, and the exchangeability of their interlayer anions [21–24]. In our previous report, we prepared an LDH-hosted chromium complex, which was an active catalyst for the oxidation reaction of GLY to DHA with 3% H_2O_2 [17]. However, the structure-performance relationship of the catalyst was unclear. In the present investigation, we further prepared a series of LDH-hosted chromium complexes with different Schiff base ligands, metal centers and loadings of active complexes. Their catalytic performance was investigated extensively in the oxidation conversion of GLY using 3% H_2O_2 as an oxidant. The effect of the structures, the composition of the catalysts, and the oxidation reaction conditions on the catalytic performance of the catalysts was discussed in detail.

2. Results and Discussion

2.1. Characterization of Catalysts

The results of elemental analysis revealed that the molar ratios of N to the transition metal in LDH-hosted complexes were in conformance with the calculated values according to Scheme 1 (see Table 1). This indicated that the obtained catalysts had the expected elemental composition.

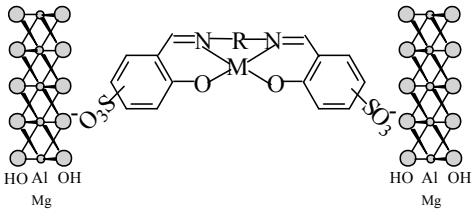

M: transition metal (Cr, Mn, Fe, Co, Cu)

(a) R=$(CH_2)_2$, (b) R=$(CH_2)_3$, (c) R=  , (d) R= 

Scheme 1. Structure schematic diagram of LDH (layered-double hydroxides)-hosted complexes: (**a**) LDH-[M(SO_3-salen)], (**b**) LDH-[M(SO_3-salan)], (**c**) LDH-[M(SO_3-sahen)], (**d**) LDH-[M(SO_3-salphen)].

Table 1. Components, textural parameters and spectroscopic data of catalysts.

Samples	Elemental Analysis Data (wt %)									S_{BET} (m^2g^{-1})	FTIR Data (cm^{-1})
	C	H	O	N	S	Mg	Al	M [a]	N/M [b]		
LDH-[C_6H_5COO]	20.24	4.23	39.65	-	-	20.36	6.52	-	-	80.2	-
LDH-[Cr(SO_3-salen)]	25.62	3.17	36.71	3.44	7.83	12.66	4.21	6.36	2.01 (2.00)[c]	66.5k	1621, 1529, 1112, 1034, 597, 418
LDH-[Cr(SO_3-salan)]	24.79	3.14	40.64	3.40	7.78	10.53	3.40	6.32	1.99 (2.00)	64.2	1620, 1522, 1110, 1035, 611, 476
LDH-[Cr(SO_3-sahen)]	29.03	3.25	36.80	3.38	7.74	10.19	3.32	6.29	2.00 (2.00)	59.6	1620, 1519, 1112, 1035, 602, 535
LDH-[Cr(SO_3-salphen)]	29.07	3.41	36.36	3.39	7.75	10.25	3.47	6.30	1.99 (2.00)	57.5	1624, 1520, 1114, 1039, 605, 412
LDH-[Mn(SO_3-salphen)]	26.52	3.16	39.17	3.10	7.07	11.34	3.55	6.09	2.00 (2.00)	60.2	1625, 1520, 1115, 1035, 602, 418
LDH-[Fe(SO_3-salphen)]	24.06	3.20	42.14	2.81	6.41	12.20	3.62	5.56	2.02 (2.00)	59.0	1620, 1518, 1110, 1035, 601, 417
LDH-[Co(SO_3-salphen)]	21.32	3.12	44.73	2.47	5.68	13.45	3.85	5.18	2.01 (2.00)	59.7	1622, 1519, 1112, 1036, 600, 420
LDH-[Cu(SO_3-salphen)]	20.02	3.08	46.26	2.33	5.22	13.71	4.05	5.33	2.00 (2.00)	58.5	1624, 1520, 1115, 1040, 610, 415

[a] The active transition metal centers in LDH (layered-double hydroxides)-hosted complex catalysts; [b] The molar ratio of N to transition metal; [c] The theoretical values.

The FTIR spectra of LDH-[C_6H_5COO], Cr(SO_3-salphen) and LDH-[Cr(SO_3-salphen)] are typically illustrated in Figure 1, and the important diagnostic bands of the other LDH-hosted complexes were also assigned, as listed in Table 1. Cr(SO_3-salphen) exhibited $\upsilon_s(SO_3^-)$ and $\upsilon_{as}(SO_3^-)$ at about 1039 and 1114 cm^{-1}, respectively. Simultaneously, the bands at about 1624 and 1520 cm^{-1} could be due to υ(C=N) and υ(C–O), and the bands at about 605 and 412 cm^{-1} were associated with υ(Cr–O) and υ(Cr–N), respectively [25–27]. This indicated that the homogeneous complex had been prepared successfully. For the LDH-hosted complexes, almost all the above characteristic bands were observed clearly though they turned relatively weaker because of their low concentration, confirming that the transition metal complex was intact during intercalation. Furthermore, compared to LDH-[C_6H_5COO], the band of $C_6H_5COO^-$ at about 1550 cm^{-1} was absent in the FTIR spectrum of the LDH-hosted complexes [25], further suggesting that the homogeneous complexes had been intercalated into the LDH interlayer by ion exchange.

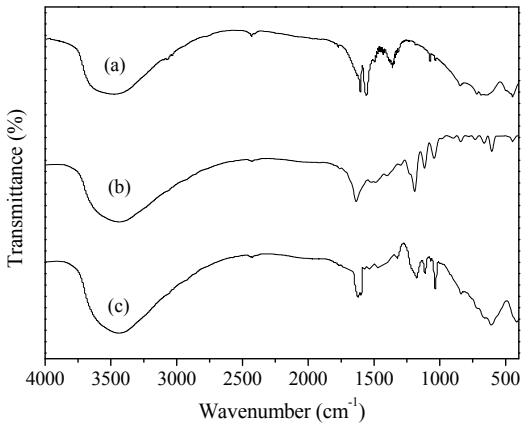

Figure 1. FTIR spectra of (**a**) LDH-[C_6H_5COO] (layered-double hydroxides), (**b**) Cr(SO_3-salphen), (**c**) LDH-[Cr(SO_3-salphen)].

XRD patterns of LDH-[C_6H_5COO] and LDH-[*M*(SO_3-salphen)] (*M*: Cr, Mn, Fe, Co, Cu) are typically illustrated in Figure 2. The samples all showed three sharp characteristic peaks of the (003), (006) and (110) planes, indicating the generation of a hydrotalcite-like structure [25,28–30]. Compared to the parent LDH-[C_6H_5COO], the (003) peaks of LDH-hosted complexes shifted to lower 2θ angles, which could be attributed to the increased interlayer distance originating from the large anion size of Schiff base complexes compared to that of $C_6H_5COO^-$.

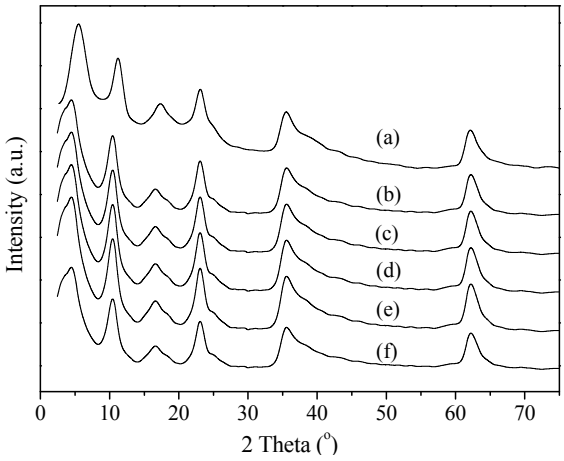

Figure 2. XRD patterns of (**a**) LDH-[C_6H_5COO], (**b**) LDH-[Cr(SO_3-salphen)], (**c**) LDH-[Mn(SO_3-salphen)], (**d**) LDH-[Fe(SO_3-salphen)], (**e**) LDH-[Co(SO_3-salphen)], (**f**) LDH-[Cu(SO_3-salphen)].

The N_2 sorption isotherms of LDH-hosted complexes in Figure 3 showed type IV isotherms, indicating the formation of mesopores due to the aggregation of particles. Moreover, compared to their parent LDH-[C_6H_5COO], LDH-hosted complexes exhibited a significantly decreased surface area (see Table 1), which might be related to the intercalation of chromium complexes into the interlayer of LDH. In addition, typically, the SEM image of LDH-[Cr(SO_3-salphen)] is shown in Figure 4, and globular-type agglomerated crystals were found due to the introduction of transition metal complexes.

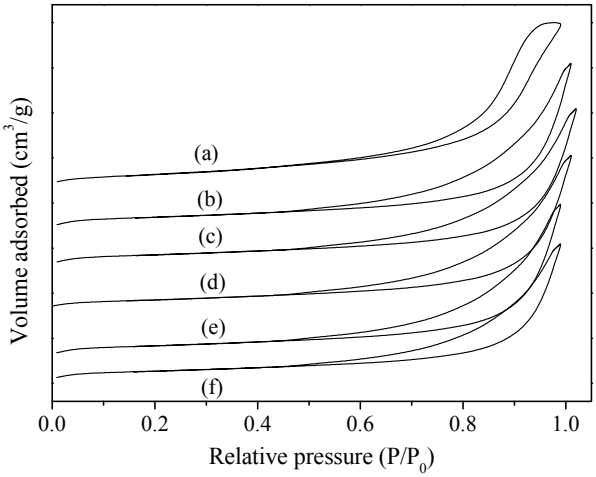

Figure 3. N_2 sorption isotherms of (**a**) LDH-[C_6H_5COO], (**b**) LDH-[Cr(SO_3-salphen)], (**c**) LDH-[Mn(SO_3-salphen)], (**d**) LDH-[Fe(SO_3-salphen)], (**e**) LDH-[Co(SO_3-salphen)], (**f**) LDH-[Cu(SO_3-salphen)].

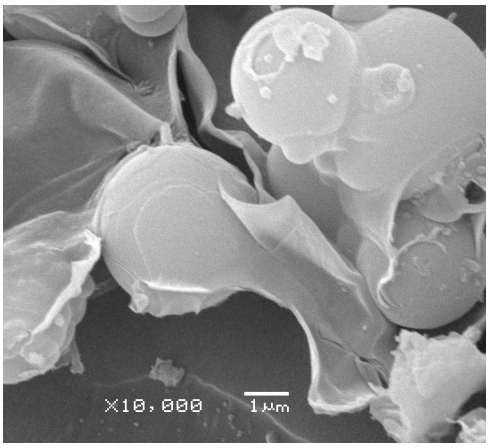

Figure 4. SEM image of LDH-[Cr(SO_3-salphen)].

2.2. Catalytic Performance

In the absence of solvent and additive, the as-prepared catalysts were used in the selective oxidation of GLY using 3% H_2O_2 as an oxidant, and the results are listed in Table 2. It was found that no product was detected without catalyst, while LDH also exhibited a slight catalytic performance (see Entry 1~2). Over homogeneous catalysts, the GLY conversion increased significantly, but the main product was the over-oxidation product of formic acid (see Entry 3~6). Upon the homogeneous complexes being intercalated into LDH, the catalytic performance, especially the selectivity to DHA (a C_3 oxygenated product of secondary alcohol) was further improved sharply (see Entry 7~17). Moreover, their catalytic performance increased with the loading of the neat complexes until the chromium content reached 6.30%; however, with the further increase in the loading of the neat complexes, the catalytic performance decreased (see Entry 10~13). It had been accepted that

homogeneous complexes tended to deactivate due to the formation of dimers or oligomers originating from their high local concentration of active complexes [31]. Thus, such obviously enhanced catalytic performance over the heterogenized catalysts could be attributed to the dispersion effect of the support.

Moreover, the LDH-hosted chromium catalysts with different Schiff base ligands were also found to show significant differences in their catalytic performance (see Entry 7~10 in Table 2). Based on the DHA yield, the catalytic performance of LDH-hosted complexes follows the trend of LDH-[Cr(SO_3-salphen)] > LDH-[Cr(SO_3-salen)] > LDH-[Cr(SO_3-salan)] > LDH-[Cr(SO_3-sahen)]. The relatively higher catalytic performance of LDH-[Cr(SO_3-salphen)] could be attributed to its bridge groups of phenyl groups, which led to the presence of π-extended coordination structures and the decrease in the system energy. Thus, the reactants and oxidant were easy to access at catalytic active sites. The worst catalytic performance over LDH-[Cr(SO_3-sahen)] might be related to the chair conformation of the cyclohexyl bridge groups, which induced high steric encumbrance around the active center.

Table 2. Catalytic performance of catalysts in GLY (glycerol) oxidation with 3% H_2O_2 [a].

Entry	Catalysts	M [b] (wt %)	GLY Con. (mol%)	Sel. (mol%)					
				DHA	Glyceric Acid	Tartronic Acid	Hydroxypyruvic Acid	Formic Acid	Oxalic Acid
1	Blank	-	0	0	0	0	0	0	0
2	LDH	-	6.4	0	1.6	0.2	0	92.6	5.6
3	Cr(SO_3-salen)	11.50	36.1	9.5	13.7	0.8	0	75.8	0.2
4	Cr(SO_3-salan)	11.15	35.5	10.2	13.6	1.2	0	69.8	5.2
5	Cr(SO_3-sahen)	10.23	30.2	10.5	7.3	1.6	5.5	70.5	4.6
6	Cr(SO_3-salphen)	10.35	38.5	7.9	11.8	2.5	2.3	73.6	1.9
7	LDH-[Cr(SO_3-salen)]	6.36	71.3	43.5	20.9	0	0	35.2	0.4
8	LDH-[Cr(SO_3-salan)]	6.32	69.4	45.7	12.0	2.0	2.5	32.1	5.7
9	LDH-[Cr(SO_3-sahen)]	6.29	48.0	22.1	14.2	3.5	12.0	38.0	10.2
10	LDH-[Cr(SO_3-salphen)]	5.65	60.0	38.6	12.3	3.2	9.5	29.6	6.8
11		6.05	75.2	46.5	13.5	2.9	6.7	28.9	7.5
12		6.30	80.8	52.5	11.6	1.9	3.8	23.7	6.5
13		6.75	57.5	40.1	11.5	2.2	5.6	31.4	9.2
14	LDH-[Mn(SO_3-salphen)]	6.29	29.4	3.7	0.9	7.0	25.5	12.1	50.8
15	LDH-[Fe(SO_3-salphen)]	6.30	45.0	38.1	9.2	6.5	20.4	10.4	15.4
16	LDH-[Co(SO_3-salphen)]	6.30	63.8	40.4	10.6	1.9	3.8	19.8	24.5
17	LDH-[Cu(SO_3-salphen)]	6.35	58.0	41.5	9.5	2.2	5.0	19.5	22.3

[a] Reaction conditions: GLY (25 mL 0.4 mol L^{-1} aqueous solution), 3% H_2O_2 (25 mL), heterogenized catalyst (0.2 g) or homogeneous catalyst (2 mol % relative to GLY), 60 °C, 4 h; [b] M: the active transition metal center in LDH-hosted complex catalysts.

The catalytic roles of the metal centers were also investigated. The results in Table 2 (Entry 10~17) and Figure 5 revealed that the type of metal cation remarkably influenced the catalytic performance of the catalysts. The GLY conversion decreased over the catalysts: LDH-[Cr(SO_3-salphen)] > LDH-[Co(SO_3-salphen)] > LDH-[Cu(SO_3-salphen)] > LDH-[Fe(SO_3-salphen)] > LDH-[Mn(SO_3-salphen)], which was almost identical to the profile of H_2O_2 efficiency. This indicated that the catalytic performance of LDH-hosted complexes was probably related to their H_2O_2 efficiency. In our previous report, we found that O_2 could not oxidize GLY in the presence of an LDH-hosted complex and base-free reaction conditions, and the disproportionation decomposition of H_2O_2 to O_2 was unproductive for GLY oxidation [17]. Thus, the remarkably low catalytic performance of LDH-[Mn(SO_3-salphen)] and LDH-[Fe(SO_3-salphen)] could be related to their especially high activities to the disproportionation decomposition of H_2O_2. For the other three LDH-hosted complexes, the different catalytic performances were attributed mainly to the increased number of electrons in the three-dimensional (3D) electron orbital from Cr to Cu. Such an increase led to the decrease in the capacity of the metal centers to accept electrons of Schiff base ligands, and then to the decrease in the ability of catalysts to activate H_2O_2. Thus, the catalysts with metal centers from Cr to Cu exhibited gradually decreased H_2O_2 efficiency and GLY conversion.

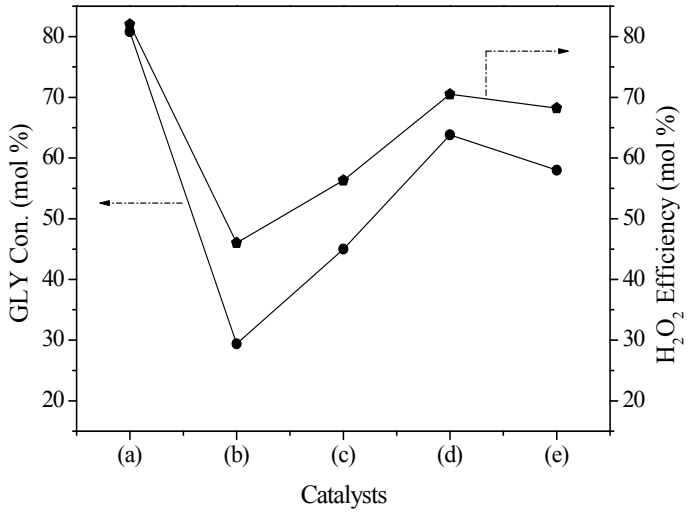

Figure 5. The GLY conversion and H_2O_2 efficiency over different catalysts: (**a**) LDH-[Cr(SO_3-salphen)], (**b**) LDH-[Mn(SO_3-salphen)], (**c**) LDH-[Fe(SO_3-salphen)], (**d**) LDH-[Co(SO_3-salphen)], (**e**) LDH-[Cu(SO_3-salphen)] Efficiency of H_2O_2 = (moles of H_2O_2 converted to the products/moles of H_2O_2 consumed) × 100.

The reaction conditions were further optimized to get the best reaction results with LDH-[Cr(SO_3-salphen)] used as the representative catalyst. It was found that the dosage of oxidant and catalyst, the reaction temperature and time all played important roles in the catalytic performance of the obtained LDH-hosted complex catalyst (see Figure 6). With the increase of the reaction time and temperature as well as the oxidant dosage, the glycerol conversion increased continuously, probably because the contact probability of the reactants and oxidant to the active sites of the catalyst increased gradually in the present heterogenized catalytic system. However, excessive time, temperature and oxidant dosage exhibited an adverse effect on DHA selectivity, indicating the presence of over-oxidation. Interestingly, the GLY conversion and DHA selectivity both increased firstly and then decreased with the increase of the catalyst dosage. This indicated that excessive catalyst was unfavorable to the oxidation reaction due to the increased diffusion resistance and the resultant decreased accessibility of reactants to the active centers of the catalyst. Under the optimal reaction conditions (10 mmol GLY, 0.2 g catalyst, 30 mL 3% H_2O_2, 6 h and 60 °C), the best GLY conversion and DHA selectivity reached 85.0% and 56.5%, respectively. The present reaction results were better than the best results in the bibliography under the solvent and base-free conditions (GLY conversion of 71.3% and DHA selectivity of 43.5% reported by us previously [17]).

The reusability of heterogenized catalyst is another important performance evaluation index with the exception of its catalytic activity. Here, after the first catalytic run, the representative catalyst of LDH-[Cr(SO_3-salphen)] was centrifugally separated from the reaction mixture, washed with water, and dried at 100 °C overnight. Then, the recovered catalyst was further used in another 10 catalytic runs, and only a slightly decreased catalytic performance was detected (see Figure 7). Elemental analysis showed that the chromium content in the recovered catalyst after 10 runs (Cr wt %: 6.30) was almost the same as the fresh catalyst (see Table 1), suggesting that no significant leaching of active metal was present. Thus, the LDH-hosted complex was a stable heterogenized catalyst for the selective oxidation of GLY.

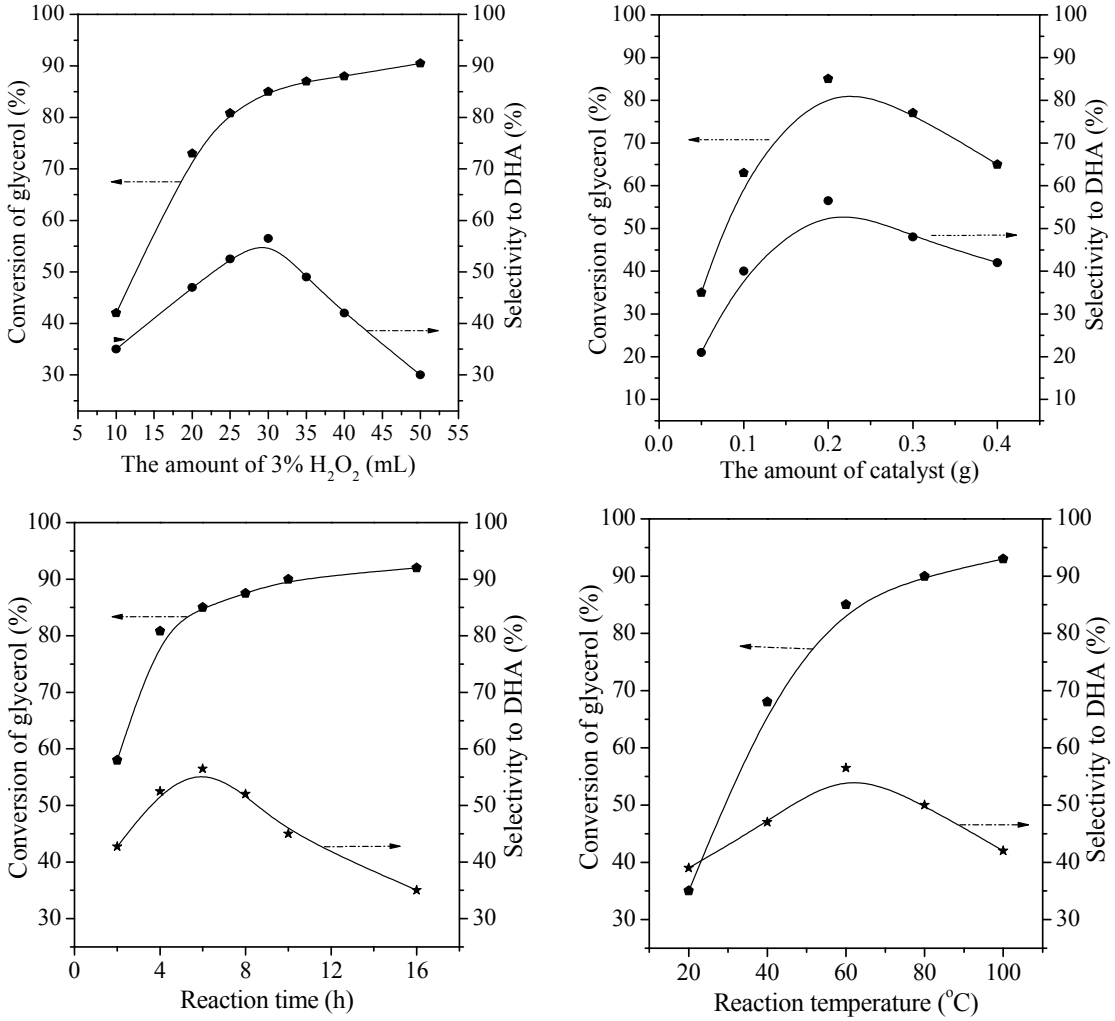

Figure 6. Effect of the reaction conditions on the catalytic performance of LDH-[Cr(SO_3-salphen)].

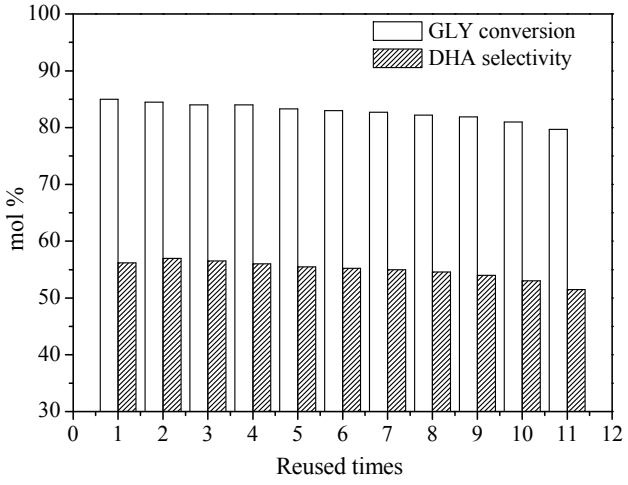

Figure 7. Reusability of LDH-[Cr(SO_3-salphen)]. Reaction conditions: GLY (25 mL 0.4 mol L^{-1} aqueous solution), 3% H_2O_2 (30 mL), catalyst (0.2 g), 60 °C, 6 h.

3. Experimental Section

3.1. Catalyst Preparation

According to the similar preparation process of LDH-hosted Cr(salen) complexes in our previous reports [17,25], here a series of LDH-hosted transition metal complexes were further synthesized by changing the kinds of ligands and metal centers (see Scheme 1). Basically, the Schiff base ligands were prepared firstly by the condensation reaction of salicylaldehyde and different diamines (ethyldiamine, propane diamine, hexamethylene diamine and o-phenylenediamine), and the molar ratio of salicylaldehyde and amines was 2. Then, the obtained Schiff base ligands were mixed with concentrated sulfuric acid to synthesize the sulphonated ligands, and the mass ratio of ligands to sulfuric acid was 5. Moreover, the ion exchange reaction was performed between the sulfonated ligands and the prepared Mg-Al LDH containing $C_6H_5COO^-$ anions in advance. Furthermore, the solid products were added into the aqueous solution of metallic salts ($MnCl_2 \cdot 4H_2O$, $FeCl_3 \cdot 6H_2O$, $CrCl_3 \cdot 6H_2O$, $NiCl_2 \cdot 6H_2O$, $CuCl_2 \cdot 6H_2O$) under stirring and N_2 atmosphere to obtain the LDH hosted transition metal complexes.

3.2. Characterization

The C, H, O, N and S contents of samples were detected on Vario EL analyzer (Elementar, Hannover, DE-NI, Germany). The contents of Mg, Al and transition metals were determined using PerkinElmer ICP OPTIMA-3000 (Thermo Electron, Waltham, MA, USA). Nitrogen sorption isotherms were measured at −196 °C on Micromeritics ASAP-2000 (Micromeritics, Norcross, GA, USA) by static adsorption procedures, and surface areas were obtained by the BET method. Powder X-ray diffraction (XRD) experiments were tested under ambient condition on Rigaku D Max III VC (Rigaku, Tokyo, Japan) using a Cu target with a Ni filter in a 2θ range of 5°–70° at 30 mA and 50 kV. The Fourier transform infrared (FTIR) spectra were gained on Bruker Tensor-27 FTIR spectrophotometer (Bruker, Ettlingen, DE-BW, Germany). SEM experiments were performed on JEOL JSM-7600F microscope (Hitachi, Akishima, Japan).

3.3. Catalytic Test

At atmospheric pressure, the GLY oxidation was carried out in a 100 mL three neck flask equipped with a constant temperature magnetic agitator (DF-II) (Shengwei, Jintan, China). Typically, a certain amount of catalyst was suspended in 25 mL aqueous glycerol solution (0.4 mol L^{-1}). The above mixture was heated to the required temperature, and then 3% H_2O_2 was cautiously added, dropwise. After the reaction was performed for a desired time, catalyst was removed by centrifugal separation. The residual aqueous solution was neutralized by adding sulfuric acid, and then was send to a high performance liquid chromatography (Agilent, Santa Clara, CA, USA) with UV-vis detectors and refractive index. H_2O_2 consumption was determined by iodometry after the reactions. Aminex HPX-87H column (Bio-Rad) (Bio-Rad, Philadelphia, PA, USA) was used for product seperation at 333 K with H_2SO_4 (0.01 mol/L, 0.5 mL/min) as eluent flowing. A 10 μL injection and a 30 min measure time were need. The calibration curves and retention times were determined using the standard samples with known concentrations.

4. Conclusions

LDH-hosted complex catalysts were found to be effective catalysts for the GLY oxidation reaction. Moreover, the metal centers, the Schiff base ligands, the loading of complexes on the support and the reaction conditions significantly influenced the performance of the catalysts. In the presence of 3% H_2O_2, the main product was C_3 oxygenated products of secondary alcohol, DHA. The GLY conversion and DHA selectivity reached 85.0% and 56.5%, respectively, over LDH-[Cr(SO_3-salphen)] which exhibited the highest H_2O_2 efficiency.

Acknowledgments: The authors acknowledge the financial supports from the National Natural Science Foundation of China (21003073, 21203093), the Natural Science Foundation of Jiangsu Province (BK20141388, BK20161481), the Qing Lan Project of Jiangsu Province, the Academic Talents Training Project of Nanjing Institute of Technology, and the College students practice innovation training program of Jiangsu Province.

Author Contributions: W.G.D. and W.X.L. designed the experiments; W.X.L. analyzed the data and wrote the paper; S.C.X., L.X.F. and L.H. performed the experiments.

Conflicts of Interest: The authors declare no conflict of interest.

References

1. Zhou, C.H.; Beltramini, J.N.; Lin, C.X.; Xu, Z.P.; Lu, G.Q.; Tanksale, A. Selective oxidation of biorenewable glycerol with molecular oxygen over Cu-containing layered double hydroxide-based catalysts. *Catal. Sci. Technol.* **2011**, *1*, 111–122. [CrossRef]
2. Brett, G.L.; He, Q.; Hammond, C.; Miedziak, P.J.; Dimitratos, N.; Sankar, M.; Herzing, A.A.; Conte, M.; Lopez-Sanchez, J.A.; Kiely, C.J.; et al. Selective oxidation of glycerol by highly active bimetallic catalysts at ambient temperature under base-free conditions. *Angew. Chem. Int. Ed.* **2011**, *50*, 1–4. [CrossRef] [PubMed]
3. Xiang, Y.Z.; Davis, R.J. Glycerol-intercalated Mg-Al hydrotalcite as a potential solid base catalyst for transesterification. *Clays Clay Miner.* **2010**, *58*, 475–485.
4. Zhou, C.H.; Beltramini, J.N.; Fan, Y.X.; Lu, G.Q. Chemoselective catalytic conversion of glycerol as a biorenewable source to valuable commodity chemicals. *Chem. Soc. Rev.* **2008**, *37*, 527–549. [CrossRef] [PubMed]
5. Prati, L.; Villa, A.; Chan-Thaw, C.E.; Arrigo, R.; Wang, D.; Su, D.S. Gold catalyzed liquid phase oxidation of alcohol: The issue of selectivity. *Faraday Discuss.* **2011**, *152*, 353–365. [CrossRef] [PubMed]
6. Tsuji, A.; Rao, K.T.V.; Nishimura, S.; Takagaki, A.; Ebitani, K. Selective oxidation of glycerol by using a hydrotalcite-supported platinum catalyst under atmospheric oxygen pressure in water. *ChemSusChem* **2011**, *4*, 542–548. [CrossRef] [PubMed]
7. Wang, F.F.; Shao, S.; Liu, C.L.; Xu, C.L.; Yang, R.Z.; Dong, W.S. Selective oxidation of glycerol over Pt supported on mesoporous carbon nitride in base-free aqueous solution. *Chem. Eng. J.* **2015**, *264*, 336–343. [CrossRef]
8. Zhang, M.Y.; Nie, R.F.; Wang, L.; Shi, J.J.; Du, W.C.; Hou, Z.Y. Selective oxidation of glycerol over carbon nanofibers supported Pt catalysts in a base-free aqueous solution. *Catal. Commun.* **2015**, *59*, 5–9. [CrossRef]
9. Zope, B.N.; Hibbitts, D.D.; Neurock, M.; Davis, R.J. Reactivity of the gold/water interface during selective oxidation catalysis. *Science* **2010**, *330*, 74–77. [CrossRef] [PubMed]
10. Sankar, M.; Dimitratos, N.; Knight, D.W.; Carley, A.F.; Tiruvalam, R.; Kiely, C.J.; Thomas, D.; Hutchings, G.J. Oxidation of glycerol to glycolate by using supported gold and palladium nanoparticles. *ChemSusChem* **2009**, *2*, 1145–1151. [CrossRef] [PubMed]
11. Kapkowski, M.; Bartczak, P.; Korzec, M.; Sitko, R.; Szade, J.; Balin, K.; Lelątko, J.; Polanski, J. SiO_2-, Cu-, and Ni-supported Au nanoparticles for selective glycerol oxidation in the liquid phase. *J. Catal.* **2014**, *319*, 110–118. [CrossRef]
12. Rodrigues, E.G.; Pereira, F.R.; Chen, X.W.; Delgado, J.J.; Orfao, J.J.M. Selective oxidation of glycerol over platinm-based catalysts supported on carbon nanotubes. *Ind. Eng. Chem. Res.* **2013**, *52*, 17390–17398. [CrossRef]
13. Shul'pin, G.B.; Kozlov, Y.N.; Shul'pina, L.S.; Strelkova, T.V.; Mandelli, D. Oxidation of reactive alcohols with hydrogen peroxide catalyzed by manganese complexes. *Catal. Lett.* **2010**, *138*, 193–204. [CrossRef]
14. McMorn, P.; Roberts, G.; Hutchings, G.J. Oxidation of glycerol with hydrogen peroxide using silicalite and aluminophosphate catalysts. *Catal. Lett.* **1999**, *63*, 193–197. [CrossRef]
15. Savanur, A.P.; Nandibewoor, S.T.; Chimatadar, S.A. Manganese (II) catalysed oxidation of glycerol by cerium (IV) in aqueous sulphuric acid medium: a kinetic and mechanistic study. *Transition Met. Chem.* **2009**, *34*, 711–718. [CrossRef]
16. Oliveira, L.C.A.; Portilho, M.F.; Silva, A.C.; Taroco, H.A.; Souza, P.P. Modified niobia as a bifunctional catalyst for simultaneous dehydration and oxidation of glycerol. *Appl. Catal. B Envioron.* **2012**, *117*, 29–35. [CrossRef]

17. Wang, X.L.; Wu, G.D.; Wang, F.; Ding, K.Q.; Zhang, F.; Liu, X.F.; Xue, Y.B. Base-free selective oxidation of glycerol with 3% H_2O_2 catalyzed by sulphonato-salen-chromium (III) intercalated LDH. *Catal. Commun.* **2012**, *28*, 73–76. [CrossRef]
18. Crotti, C.; Farnetti, E. Selective oxidation of glycerol catalyzed by iron complexes. *J. Mol. Catal. A Chem.* **2015**, *396*, 353–359. [CrossRef]
19. Oliveira, V.L.; Morais, C.; Servat, K.; Napporn, T.W.; Tremiliosi-Filho, G.; Kokoh, K.B. Glycerol oxidation on nickel based nanocatalysts in alkaline medium–Identification of the reaction products. *J. Electroanal. Chem.* **2013**, *703*, 56–62. [CrossRef]
20. Wu, G.D.; Wang, X.L.; Huang, Y.A.; Liu, X.F.; Zhang, F.; Ding, K.Q.; Yang, X.L. Selective oxidation of glycerol with O_2 catalyzed by low-cost CuNiAl hydrotalcites. *J. Mol. Catal. A Chem.* **2013**, *379*, 185–191. [CrossRef]
21. Urdă, A.; Popescu, I.; Cacciaguerra, T.; Tanchoux, N.; Tichit, D.; Marcu, I.C. Total oxidation of methane over rare earth cation-containing mixed oxides derived from LDH precursors. *Appl. Catal. A Gen.* **2013**, *464–465*, 20–27. [CrossRef]
22. Dobrosza, I.; Jiratovab, K.; Pitchon, V.; Rynkowski, J.M. Effect of the preparation of supported gold particles on the catalytic activity in CO oxidation reaction. *J. Mol. Catal. A Chem.* **2005**, *234*, 187–197. [CrossRef]
23. Varga, G.; Ziegenheim, S.; Muráth, S.; Csendes, Z.; Kukovecz, A.; Kónya, Z.; Carlson, S.; Korecz, L.; Varga, E.; Pusztai, P.; et al. Cu(II)-amino acid–CaAl-layered double hydroxide complexes, recyclable, efficient catalysts in various oxidative transformations. *J. Mol. Catal. A Chem.* **2016**, *423*, 49–60. [CrossRef]
24. Lv, W.M.; Yang, L.; Fan, B.B.; Zhao, Y.; Chen, Y.F.; Lu, N.Y.; Li, R.F. Silylated MgAl LDHs intercalated with MnO_2 nanowires: Highly efficient catalysts for the solvent-free aerobic oxidationof ethylbenzene. *Chem. Eng. J.* **2015**, *263*, 309–316. [CrossRef]
25. Wu, G.D.; Wang, X.L.; Li, J.P.; Zhao, N.; Wei, W.; Sun, Y.H. A new route to synthesis of sulphonato-salen-chromium (III) hydrotalcites: Highly selective catalysts for oxidation of benzyl alcohol to benzaldehyde. *Catal. Today* **2008**, *131*, 402–407. [CrossRef]
26. Choudary, B.M.; Ramani, T.; Maheswaran, H.; Prashant, L.; Ranganath, K.V.S.; Kumarb, K.V. Catalytic asymmetric epoxidation of unfunctionalised olefins using silica, LDH and resin-supported sulfonato-Mn (salen) complex. *Adv. Synth. Catal.* **2006**, *348*, 493–498. [CrossRef]
27. Bhattacharjee, S.; Anderson, J.A. Comparison of the epoxidation of cyclohexene, dicyclopentadiene and 1,5-cyclooctadiene over LDH hosted Fe and Mn sulfonato-salen complexes. *J. Mol. Catal. A Chem.* **2006**, *249*, 103–110. [CrossRef]
28. Cantrell, D.G.; Gillie, L.J.; Lee, A.F.; Wilson, K. Structure-reactivity correlations in MgAl hydrotalcite catalysts for biodiesel synthesis. *Appl. Catal. A Gen.* **2005**, *287*, 183–190. [CrossRef]
29. Zhou, H.; Zhuo, G.L.; Jiang, X.Z. Heck reaction catalyzed by Pd supported on LDH-F hydrotalcite. *J. Mol. Catal. A Chem.* **2006**, *248*, 26–31. [CrossRef]
30. Cavani, F.; Trifiro, F.; Vaccari, A. Hydrotalcite-type anionic clays: Preparation, properties and applications. *Catal. Today* **1991**, *11*, 173–301. [CrossRef]
31. Karandikar, P.; Dhanya, K.C.; Deshpande, S.; Chandwadkar, A.J.; Sivasanker, S.; Agashe, M. Cu/Co-salen immobilized MCM-41: characterization and catalytic reactions. *Catal. Commun.* **2004**, *5*, 69–74. [CrossRef]